[redacted]

CONF-870413--2

LA-UR-87-1878

JUL 1 ? 1987

Los Alamos National Laboratory is operated by the University of California for the United States Department of Energy under contract W-7405-ENG-36

LA-UR--87-1878

DE87 011791

TITLE: SUMMARY SESSION--FUTURE DIRECTIONS IN INTERPLAYS BETWEEN PARTICLE AND NUCLEAR PHYSICS

AUTHOR(S): Gerald Thomas GARVEY

SUBMITTED TO: To be included in published Proceedings of
XIth International Conference on Particles and Nuclei (PANIC 87)
Kyoto, Japan
April 20-24, 1987

DISCLAIMER

MASTER

Los Alamos Los Alamos National Laboratory
Los Alamos, New Mexico 87545

SUMMARY SESSION
FUTURE DIRECTIONS IN INTERPLAYS BETWEEN PARTICLE AND NUCLEAR PHYSICS

Gerald T. Garvey
Los Alamos National Laboratory—LAMPF
MS H836, Los Alamos, NM 87545

A summary talk that also attempts to look to the future presents a difficult task indeed. Let me begin this one with a general prognosis on searches for rare decays forbidden in the Standard Model (SM). The quest for new physics that will clearly signal the need to extend the present minimal version of the SM is the principle motivating force in most of today's forefront particle physics research. Direct production of new bosons or fermions is principally governed by the available center of mass energy. Figure 1 shows the famous Livingston plot of accelerator energy as a function of time. Note that beginning around 1975 the energy of the colliders is expressed in terms of the accelerator energy for an equivalent fixed target facility. The slope of the historical trend line shows a very impressive factor of 10 increase every 6 years. This is somewhat of an exaggeration as

$$\sqrt{s} = 2E_c = \sqrt{2M_p E_L}$$

where E_c is the collider beam energy and E_L is the equivalent laboratory energy of a mythical fixed target facility. Thus, the real gain in terms of physics (neglecting the internal structure of protons) scales as $\sqrt{E_L}$ so that the real gain is on an order of magnitude every 12 years.

In a rare-decay process mediated by a heavy boson, the branching ratio for the rare process is depends on the fourth root of mass of the heavy boson (M_B).

$$B.R. \sim \left(\frac{1}{M_B^2}\right)^2 \quad . \tag{1}$$

Figure 2, due to Dick Mischke at Los Alamos, shows the impressive history of the progress made in searches for a variety of rare decays of the muon. The ambitious goal set for the

early 1990's for $\mu \rightarrow e\gamma$ is for the MEGA experiment[1] at LAMPF which aims to achieve a sensitivity equivalent to a branching ratio of 10^{-13}. The trend line of this plot shows approximately a factor of 10 increase in sensitivity every 3 years. Thus, the sensitivity to M_B in rare decay searches also increases a factor of 10 every 12 years. In spite of the relative insensitivity of M_B to the branching ratio, real improvements in detector technology, as well as increased particle fluxes, make rare decay experiments very competitive. The multidimensional nature of detector systems is the principle reason that such rapid progress is possible. Larger, finer grained detectors allow greater efficiency, better energy resolution, faster timing, better particle identification, while still allowing ever higher rate capability. As an illustration of how this leads to very large overall improvement in performance, let me take MEGA as an example. Figure 3 shows a diagram of the detector design. The entire detector is inside a large superconducting solenoidal magnet. The electrons are tracked in a central proportional drift chamber while the photons are converted to pairs in four layers of Pb and the resultant pairs are momentum analyzed in accompanying layers of drift chambers. Table I lists the many improvements in detector performance over the previous measurement[2] done at LAMPF with the Crystal Box. Table II shows the various rates that have to be contended with to obtain a sensitivity in the branching ratio of a part in 10^{13}. Though 3×10^7 muons are stopped per second, only 11 candidate events per sec have to be written to tape for further analysis. Of course, as the branching ratio gets smaller and smaller, the experiments get more difficult and expensive but not prohibitively so. MEGA will cost approximately three times it predecessor for a gain in sensitivity of 500. Thank God for microchips!

Table I. Various Properties of the MEGA Detector Illustrating the Comparative Advantages to Earlier Detectors.

Property	*MEGA*	*Crystal Box*
Fractional electron energy resolution	0.005	0.08
Fractional photon energy resolution	0.02	0.08
Photon-electron timing (ns)	0.5	1.1
Electron position resolution at the target (mm)	2.0	2.0
Electron angular resolution, including target scattering (deg)	0.6	1.3
Photon conversion point resolution (mm)	3	25
Electron-photon angle (deg)	0.6	8.0
Photon angle (deg)	10	—
Inefficiency of bremsstrahlung veto	0.2	0.5
Fractional solid angle times detection efficiency	0.1	0.2
Muon stopping rate (s^{-1})	3×10^7	5×10^5
Running time (s)	1.2×10^7	2×10^6
Branching ratio sensitivity	9×10^{-14}	4×10^{-11}
Number of background events with $\pm 2\sigma$ cuts	0.9	~50

All resolutions are FWHM.

Table II. Data Handling Rates in the MEGA Experiment.

Identifier	*Reduction Factor*	*Instantaneous Rate (Hz)*	*Average Rate (Hz)*
Muon decays		5×10^8	3×10^7
Fractional solid angle	0.7	3.5×10^8	
$E_\gamma > 37$ MeV	0.0008	2.8×10^5	
Photon conversion efficiency	0.23	6.4×10^4	
Photon area—$E_\gamma > 42$ MeV	0.5	3.2×10^4	
Microprocessor input		3.2×10^4	1.9×10^3
$E_e > 37$ MeV and $\Delta\phi_{e\gamma} < 30°$	0.5		960
$E_e > 50$ MeV and $(R\Delta\phi\Delta z)_\gamma < 16$ cm^2	0.07		64
$E_\gamma > 46$ MeV	0.33		21
$\Delta t_{e\gamma} < 5$ ns	0.3		21
Tape writing			11

The following observation has been made by H. Harari[3] and is important to pass along. Even though one can increase beam energy (as long as your government has sufficient yen) there is an ever decreasing cross section for interesting events. The particles of the Standard Model are all point particles at least up to the length scale of the unification mass and, as such, the cross section (apart from resonances) for production of new point particles falls as

$$\sigma \sim \frac{1}{E^2} \quad . \tag{2}$$

A useful reference value is

$$\sigma(e^+e^- \rightarrow \mu^+\mu^-) = 10^{-39} \text{ cm}^2 \text{ at } E_{e+} + E_{,-} = 10 \text{ TeV} \quad . \tag{3}$$

Using the scaling of a factor of 10 in accelerator energy every 12 years means that on or about 2023 we can expect to see a 1 PeV (10^{15} eV) facility. The cross section for new particles at that energy is 10^{-43} cm^2 using the above relations. To obtain 10^3 events in one

year of running requires a luminosity of 10^{39} cm^{-2}sec^{-1}. With particle numbers proposed for the Stanford Linear Collider, the linear dimensions of beam would have to be reduced to 10^{-8} cms to achieve the above luminosity. Thus, rare decays look like an excellent way to probe the very highest scales.

The forbidden process $K_L^0 \rightarrow \mu e$ is now being studied at the AGS to a sensitivity that will reach 10^{-11} to 10^{-12}. Its sensitivity to a flavor violating heavy boson is

$$M_B = 20 \left[\frac{10^{-8}}{BR(K \rightarrow \mu e)} \right]^{1/4} \text{ TeV} \quad . \tag{4}$$

To be sensitive to $M_B = 1$ PeV requires a branching ratio sensitivity of 2×10^{-15}. Hence 10^8-10^9 K_0^L/sec are required, a flux achievable in the next generation kaon factories being proposed around the world. Of course, the experimentalists will have to struggle with very nasty background problems, but detector technology keeps getting better all the time. RARE DECAYS deserve much attention.

A conference that has been as extensive as this one makes it difficult for a summary speaker to find unifying themes that cut across many of the presentations and discussions. One theme that seemed to come up time and time again was the notion of broken symmetries in strongly interacting systems. Broken symmetries may indeed be the most natural way for the impact of QCD to manifest itself in the hadronic regime. Two such symmetries that are clearly broken are isospin symmetry and chiral symmetry. In the first instance, any attempt to explain the mass difference between the neutron and proton in purely electromagnetic terms always gets the proton to be heavier than the neutron. Postulating the down quark to have approximately 3 MeV more mass than the up quark solves this problem and accounts for the fact that the members of all isospin multiplets having the greatest numbers of u (or $\overline{u}$) quarks have the smallest mass. How this carries over to nuclear physics is not clear at the moment, but it has to be recalled that the mass splitting within nuclear isospin multiplets has remained an unsolved problem for some 20 years now. This problem, often referred to as the Nolen–Schiffer[4] anomaly, arises because the best

calculations which incidently use a great deal of phenomenological input systematically underpredict the observed mass splitting by approximately 10%. This effect shows up in the ^{3}H-^{3}He mass difference and persists up through the Pb-Bi region. However, isospin breaking was not much discussed at this meeting, but chiral symmetry breaking and its implications were extensively presented and discussed.

In a chirally symmetric system such as one would have in QCD with massless quarks, the vector and axial vector charges commute with the Hamiltonian

$$[Q_i, H_0] = 0 \qquad [Q_i^5, H_0] = 0 \ , \tag{5}$$

where Q_i and Q_i^5 are the vector and axial vector charges and the subscripts i refer to the indices $1 \ldots 8$ that occur in SU(3) of flavor. As vector gluon interactions conserve chiral symmetry, chiral symmetry breaking is ascribed to finite quark masses. Hence, we have

$$H = H_0 + H^1 \tag{6}$$

where

$$H^1 = m_u \bar{u}u + m_d \bar{d}d + m_s \bar{s}s \ . \tag{7}$$

This term can be rewritten as an SU(3) singlet plus an SU(3) octet term. Recall that chiral symmetry and PCAC are intimately related via

$$\frac{\partial A_\pi^\mu}{\partial X_\mu} = m_\pi^2 f_\pi \phi_\pi = -\frac{\epsilon_0}{\sqrt{3}}(\sqrt{2} + C)v_\pi \ . \tag{8}$$

The limit $m_\pi^2 \to 0$ corresponds to the limit of $C = -\sqrt{2}$ where $C = \epsilon_8/\epsilon_0$, the ratio of the expectation values of the symmetry breaking octet term to the singlet term.

Let's look at some of the consequences of chiral symmetry on hadronic processes. In the limit $m_\pi^2 \to 0$ PCAC leads to the Goldberger–Tremain relation for the axial vector decay constant of the neutron.

$$g_A^{\text{theory}}(0) = \frac{f_\pi f_{\pi NN}(0)}{m_N} \tag{9}$$

In this prediction the effects of chiral symmetry breaking are not included. A recent calculation[5] shows that they are small and can be written as

$$g_A^{\text{theory}}(0) = \frac{f_\pi f_{\pi NN}(0)}{m_N}(1+d) \tag{10}$$

where a calculation of chiral symmetry breaking yields $d = -0.025 \pm 0.005$. Using the most recent values for the parameters used in Eqs. (9) and (10) one has f_π (the pion decay constant) $= 93.2 \pm 0.1$ MeV, $f_{\pi NN}(q^2) \equiv f_{\pi NN}(0)\left(1/\left(1-\frac{q^2}{\Lambda^2}\right)\right)$ where $\Lambda = 1150 \pm 350$. From experiment $f_{\pi NN}(q^2 = m_\pi^2)/4\pi = 14.28 \pm 0.18$. This yields

$$g_A^{\text{theory}}(0) = 1.277 \pm 0.015$$

compared to the most recent[6] experimental value of

$$g_A^{\text{exp}} = 1.262 \pm 0.005 \quad .$$

This agreement is very satisfying and should serve to motivate improvement in the errors in both experiment and the calculation of chiral symmetry breaking. The experiments yielding the above result employ a cold neutron beam with a neutron energy of $\sim 10^{-3}$ eV.

The issue of chiral symmetry breaking appeared at this conference in the context of the pion-nucleon sigma term. In fact, apart from the supernova event and the subsequent detection of its neutrinos at Kamioka and IMB, the subject receiving the most attention at this conference is the apparently large size of the pion-nucleon sigma term ($\Sigma_{\pi N}$). The proposed consequences resulting from a large $\Sigma_{\pi N}$ are indeed remarkable, and I will list them below. Experimentally, the pion-nucleon sigma term is an extrapolation of the π-N forward scattering amplitude at low energy to $q^2 = 0$. Theoretically the sigma term may be written

$$\Sigma_{\pi N}(q^2) = \hat{m}\langle P_f \mid \bar{u}u + \bar{d}d \mid P_i\rangle \tag{11}$$

where $\hat{m} = (m_u + m_d/2)$. It is easy to show that

$$\Sigma_{\pi N}(0) = 27 \text{ MeV if } \langle P_f \mid \bar{s}s \mid P_i\rangle = 0 \quad . \tag{12}$$

However, the observed values of the pion Σ term appear to be much larger than the theoretical expectation. For example, in a recent experiment[7] $\Sigma_{\pi N}^{\rm exp}(2m_\pi^2) = 65$ MeV, which leads to $\Sigma_{\pi N}^{\rm exp}(0) = 52 \pm 2$ MeV, a factor 2 larger than expected. The experimental determination, however, is not absolutely clear and pionic atom studies[8] give a result more in accord with theoretical expectations. Assuming the large value measured in π-p scattering is correct, then chiral symmetry breaking requires that

$$\langle \bar{s}s \rangle_p = 0.25 \langle \bar{u}u + \bar{d}d \rangle_p \quad . \tag{13}$$

Such a large expectation value for the strange quark content of the proton leads to the conclusion that strange quarks contribute approximately one-third of the proton's mass. That is,

$$\begin{aligned} \Delta M_p^s = m_s \langle \bar{s}s \rangle_p &= \frac{m_s}{\hat{m}} \frac{\langle \bar{s}s \rangle_p}{\langle \bar{u}u + \bar{d}d \rangle_p} \Sigma_{\pi N} \\ &= (25)(0.25)50 M_U = 300 \text{ MeV} \end{aligned} \tag{14}$$

It should be pointed out that such a large contribution to the proton mass from strange quarks is consistent[9] with the Skyrme $SU(3)_c$ model, etc. The large value of the πN sigma term directly leads to a prediction[9,10] of a very large KN sigma term (Σ_{KN}). A recent and important paper[9] by Kaplan and Nelson shows that this large value of the KN sigma term requires the KN s-wave interaction to be sufficiently attractive that a K-N condensate is expected at about 2.7 times nucleus density. This is a surprising result and would have a large effect on the nuclear equation of state. However, as Bob Jaffe cautioned in his presentation,[11] most of these results depend on first-order perturbation theory and may not be correct. Models such as the hybrid chiral bag model where some of the strange quark contributions can come from the meson sea external to the bag do not produce such large values of Σ_{KN} and in that case the contribution of the mesons with strange quarks to the nucleon mass is only 40 MeV.

As an experimentalist I found it interesting and disconcerting that all this discussion took place without reference to the measurement of strange quarks in the nucleus via deep inelastic neutrino scattering. Charmed quarks are produced via

$$\left.\begin{aligned} \nu_\mu + d &\rightarrow \mu^- + c \\ \nu_\mu + s &\rightarrow \mu^- + c \end{aligned}\right\} \tag{15a}$$

$$\left.\begin{aligned} \overline{\nu}_\mu + \overline{d} &\rightarrow \mu^+ + \overline{c} \\ \overline{\nu}_\mu + \overline{s} &\rightarrow \mu^+ + \overline{c} \end{aligned}\right\} \tag{15b}$$

The c and $\overline{c}$ quarks decay respectively to $s + \mu^+ + \nu_\mu$ and $\overline{s} + \mu^- + \overline{\nu}_\mu$. Hence, deep inelastic neutrino scattering forming charmed quarks has a very clean signature as opposite sign muons are produced. CDHS has measured[12] the yield for these processes and their result is shown in Fig. 4.

They define

$$U \equiv \int_0^1 x\, u(x) dx \quad , \tag{16}$$

and find for the total sea

$$\overline{U} + \overline{D} + 2\overline{S} = 0.070 \pm 0.005$$

and

$$\frac{2\overline{S}}{U + D} = 0.052 \pm 0.004 \quad .$$

These results would lead one to infer that the contribution of the sea is very small in strong contradiction to the arguments previously made regarding the effects of the strange quark sea.

It is both interesting and significant to note that the experiments required to examine the issues of chiral symmetry have used cold neutrons (10^{-3} eV), low-energy pions ($T_\pi = 50$ MeV), and 400 GeV protons to produce the neutrino used in the deep inelastic scattering. Thus, a single concept has consequences over a range in energy of 10^{12} and dramatically illustrates the need for a diversity of capability.

T. Thomas, in his presentation,[13] expressed a desire for a better determination of the s quark distribution than is presently available from neutrino scattering. Figure 5 shows how poorly that distribution is determined. The $\overline{s}$ distribution is better known, and Thomas showed it was fit rather well by the cloudy bag model. Using his model for convoluting the hadron distribution into a quark distribution, the s quark distribution is predicted to be rather different than that of the $\overline{s}$ because of the role of the Σ and Λ particles which contribute to the s distribution but not $\overline{s}$. Learning how to carry out reliable convolution is clearly an essential issue if we are ever to relate QCD and hadron descriptions in a satisfactory manner. Be that as it may, it appears to me that using the Drell-Yan process with K^- would be the best way to study $s(x)$, particularly at large values of x where $\overline{u}$ contributions will be generally suppressed. If there is a long tail in x in the $s(x)$ distribution, Drell-Yan experiments with K^- beam would be the best way to find it. However, to do that will require intense K^- beams of ≥ 30 GeV.

As the Drell-Yan process[14-16] may not be familiar to many of you, I would like to take a few moments to review it and point out its potentially large impact on studying hadronic and nuclear structure. Figure 6 illustrates the fundamental Drell-Yan process. In a hard collision between two hadrons, a quark (antiquark) in the incident particle (1) annihilates with an antiquark (quark) in the target, (2) producing a virtual photon which is realized as a massive dilepton pair. The electromagnetic cross section for this process can be written as

$$\frac{d^2\sigma}{dx_1 dx_2} = \frac{4\pi\alpha^2}{9sx_1x_2} K \sum_i e_i^2 [q_i(1)\overline{q}_i(2) + \overline{q}_i(1)q_i(2)] \quad . \tag{17}$$

The sum extends over quark flavors i; x_1 and x_2 are the fractions of the hadron momentum carried by the interacting quarks; $q_i(1)$, etc., are the quark momentum distributions such as are measured in deep inelastic muon scattering. The kinematics associated with the Drell-Yan process is straightforward. The center of mass energy $\sqrt{s}$ is

$$\sqrt{s} = \sqrt{2M_p E_{\rm lab}} \quad . \tag{18}$$

The virtual photon energy is

$$E_\gamma = (x_1 + x_2)\frac{\sqrt{s}}{2} \tag{19}$$

with a $p_\parallel$ along the beam direction of

$$p_\parallel = (x_1 - x_2)\frac{\sqrt{s}}{2} \quad . \tag{20}$$

Thus,

$$M^2_{\mu\mu} = E^2_\gamma - p^2_\parallel = s x_1 x_2 \quad . \tag{21}$$

Figure 7 shows the yield[14] of dilepton pairs resulting from 400 GeV protons on Pt. The peaks in the spectra do not result from the Drell-Yan process but rather from the decay of the indicated vector mesons. This meson-produced background requires one to work in the region $4.2 \leq M_{\mu\mu} \leq 9.0$ GeV or $M_{\mu\mu} > 12$ GeV to avoid contributions from these resonances. Once the interesting region of x_1 and x_2 is specified, it is best to employ the smallest value of s that provides $M_{\mu\mu} \geq 4.2$ GeV. This makes the yield as large as possible for specific $x_1 x_2$. From a vast amount of theoretical and experimental study it is now clear that the longitudinal quark momentum distributions are not measurably affected by initial state effects as long as $M_{\mu\mu} > 4$ GeV. Recent work[17,18] has also shown that the Drell-Yan process is now quantitatively understood. For nearly a decade (up until 1985) the observed cross section was known to be a factor of 2 larger than the simple parton model given by Eq. (17) and K was set equal to approximately 2 to produce agreement with experiment. The more recent theoretical work cited above has also shown that both the K factor and anomalies noted in the transverse momentum distribution function are brought into line with experiment via QCD. Very nice examples of this improved state of affairs were provided to me at this conference by Hans Pirner.[19] Figure 8 shows a calculation by P. Chiappetta and Pirner of a Drell-Yan yield from π^- on W at $\sqrt{s} = 20$ GeV by the NA-10 collaboration at CERN. The diagram shows that the inclusion of soft gluon corrections increases the predicted parton yield by about a factor of 2 and obtains good agreement with

experiment. Figure 9 shows how the transverse momentum distribution of the dilepton pair can be accounted for, again using QCD. The good agreement at $q_T < 1$ GeV comes from multiple soft gluon exchange while the agreement out at $q_T > 2.5$ GeV comes from single hard gluon exchange which can be treated perturbatively. The intermediate region $1 \leq q_T \leq 2.5$ GeV/c is not as well accounted for.

How should one use the Drell-Yan process to learn more about nuclear medium effects? First, Eq. (17) shows that the Drell-Yan process can be flavor specific. Differently than charged lepton scattering which only is sensitive to the square of the quark charge, the Drell-Yan process, properly implemented, can identify quark type. Figure 10 shows the quark structure function for the nucleon. XF_3 is the valence quark distribution while $\overline{q}$ is the sea quark distribution function. If we use a high-energy proton beam and select $x_1 > 0.6$ then we can be sure that the annihilated quark in the proton is a valence quark; hence the object annihilated in the target must be the corresponding antiquark. Thus, one is in a position to directly compare antiquark distribution functions for any nucleus. This information may be very useful in sorting out the EMC effect and is of great interest of its own accord because of the low x behavior noted in some recent deep inelastic muon scattering results. Figure 11 shows the kinematic regions that reveal the antiquark structure function as well as the domains in x that can be probed with different energy beams. Recall that in order to have interpretable results

$$M_{\mu\mu} = \sqrt{2M_p E_L x_1 x_2} > 4.2 \text{ GeV} \quad .$$

Hence to probe small values of x_2, one needs to have very high-energy beams. Figure 12 shows the expected[20] statistical error as for $R(\overline{q})$ for an experiment to run at FNAL in comparing the antiquark distribution function in Ca to that of deuterium. Also shown is what can be achieved at 45 GeV where one is restricted to larger ($x_2 > 0.2$) values of x_2.

I hope I have shown you some of the potential power of the Drell-Yan process to yield flavor specific quark distribution functions. Insofar as a principle intellectual goal of most

of the participants at this conference is to establish the foundation of hadronic and nuclear physics on QCD, I would think this most important process should be fully exploited. Its full exploitation will require primary beam energies of 60 to 100 GeV, a good deal higher than has been discussed for kaon factories.

To summarize quickly, what does this scientific community require for the future? Figure 13 shows an artist's concept of our most recent thoughts on that matter at Los Alamos. The facility depicted[21] increases the LAMPF beam energy in a superconducting linac to 2 GeV before feeding it to two booster synchrotrons. Five hundred microamps at 2 GeV (1 megawatt of beam power) will be delivered to a spallation target at a low duty factor (12 Hz) to provide an intense cold neutron and neutrino source. Some 25 μa will be brought to 60 GeV at 6 Hz with a 50% duty factor. The span of research allowed by such a facility is staggering, and I close with a short list in Table III of the obvious opportunities it provides for nuclear physics.

Table III. Partial List of Reasons Why a High-Intensity–High-Energy ($E_p >$ 45 GeV) Facility is Required for Nuclear Physics.

(1) INTENSITY
- Higher intensity by a factor of 100 over what is available today
- Provides as many kaons per day as are currently available in the world per year

(2) PRIORITY
- Issues of importance to strong interaction physics are accorded high priority

(3) Items (1) and (2) will increase the pace of research by a factor of 2 to 5

(4) As HEP proceeds to collider physics, this will be the major facility to pursue hadron physics

(5) Flavor specific quark degrees of freedom can be directly accessed in the Drell-Yan process

(6) *If this facility is not constructed, how will this crucial part of strong interaction physics be carried out?*

References

[1] M. Cooper (Spokesperson), LAMPF Proposal No. 969 (1985).

[2] R. Bolton et al., *Physical Review Letters* **56** (1986) 2461.

[3] H. Harari, SLAC-PUB-4223, February 1987.

[4] J. A. Nolan and J. P. Schiffer, *Annual Review of Nuclear Science* **19** (1969) 471.

[5] C. A. Dominguez, *Riv. Nuovo Cimento* **6** (1985).

[6] P. Bopp et al., *Physical Review Letters* **56** (1986) 919.

[7] U. Wiedner et al., *Physical Review Letters* **58** (1987) 648.

[8] E. Bovet et al., *Physics Letters* **153B** (1985) 231.

[9] J. F. Donoghue and C. R. Nappi, *Physics Letters* **168B** (1986) 105.

[10] D. B. Kaplan and A. E. Nelson, *Physics Letters* **175B** (1986) 57.

[11] R. L. Jaffe, proceedings of this conference; and R. L. Jaffee and C. L. Korpa, to be published in *Comments on Nuclear and Particle Physics.*

[12] H. Abramowicz et al., *Zeitschrift für Physik C* **15** (1982) 19.

[13] T. Thomas, proceedings of this conference and private communication, April 1987.

[14] I. R. Kenyon, *Reports on Progress in Physics* **45** (1982) 1261.

[15] C. Grosso-Pilcher and M. J. Shocket, *Annual Review of Nuclear and Particle Science* **36** (1986) 1.

[16] E. Berger and F. Coester, to be published in *Annual Review of Nuclear and Particle Science.*

[17] G. Altarelli, R. K. Ellis, and G. Martinelli, *Physics Letters* **151B** (1985) 457.

[18] G. T. Bodwin, *Physical Review D* **31** (1985) 2616.

[19] H. Pirner, private communication, April 1987.

[20] J. Moss (Spokesman), E772, FNAL.

[21] H. A. Thiessen, Particle Accelerator Conference, March 16–19, 1987, to be published by IEEE.

Figure Captions

1. Plot of accelerator energy as a function of time.
2. Plot of the limits achieved for the branching ratios of various rare decays of the muon as a function of time.
3. Schematic diagram of the MEGA detector layout.
4. (a) Spectrum of deeply inelastic muon antineutrino events yielding oppositely charged muon pairs. It is plotted against x, the fraction of momentum carried by the struck quark (Ref. 12).
   (b) Spectrum of deeply inelastic muon neutrino events yielding oppositely charged muon pairs. This spectrum is a composite of contributions from s and d quarks (Ref. 12).
5. (a) Fit to the strange antiquark distribution function measured in muon antineutrino scattering (T. Thomas, private communication).
   (b) Fit to strange quark distribution function extracted from muon neutrino scattering (T. Thomas, private communication).
6. Diagram of the Drell-Yan process.
7. Yield of $\mu^+\mu^-$ pairs as a function of their mass. The peaks are due to the $\mu^+\mu^-$ decay of the designated vector meson.
8. Fit to the observed yield of $\mu^+\mu^-$ pairs. The lower dotted line is the predicted yield using a simple parton model. The upper dashed line is the fit obtained using QCD soft gluon exchange and rescaling as suggested by EMC experiments (H. Pirner, private communication).
9. Fit to the p_+ distribution of $\mu_+\mu_-$ pairs. The upper line takes no account of nuclear effects while the lower employs the Q^2 rescaling suggested by the EMC effect (H. Pirner, private communication).
10. Quark distribution functions for the nucleon as derived from experiment. The figure is based on data in Wohl et al., *Review of Modern Physics* 56 (1984) 51.

11. The upper lined region shows the region of the x_1x_2 plane in which the antiquark distribution function of a nuclear target (x_2) can be measured using incident energetic protons (x_1). The lower cross hatched region yields the quark distribution of target using the nucleon antiquark distribution from Fig. 10. The entire area to the right of the curves labeled by E_L (GeV) shows the available region of the x_1x_2 plane for Drell-Yan studies.
12. $R_{\bar{q}}$ is the ratio of the antiquark distribution function per nucleon for a nucleus compared to the proton. The points with large solid error bars are from neutrino experiments, while the points with smaller dashed error bars are the expected statistic error bars for an upcoming FNAL experiment at 800 GeV (Ref. 20). Also shown are the expected statistical errors for an experiment at 45 GeV.
13. Schematic layout of an advanced hadron facility at Los Alamos. Five hundred microampheres time average will be available from the 2 GeV compressor ring and 25 microampheres will be available at 60 GeV.

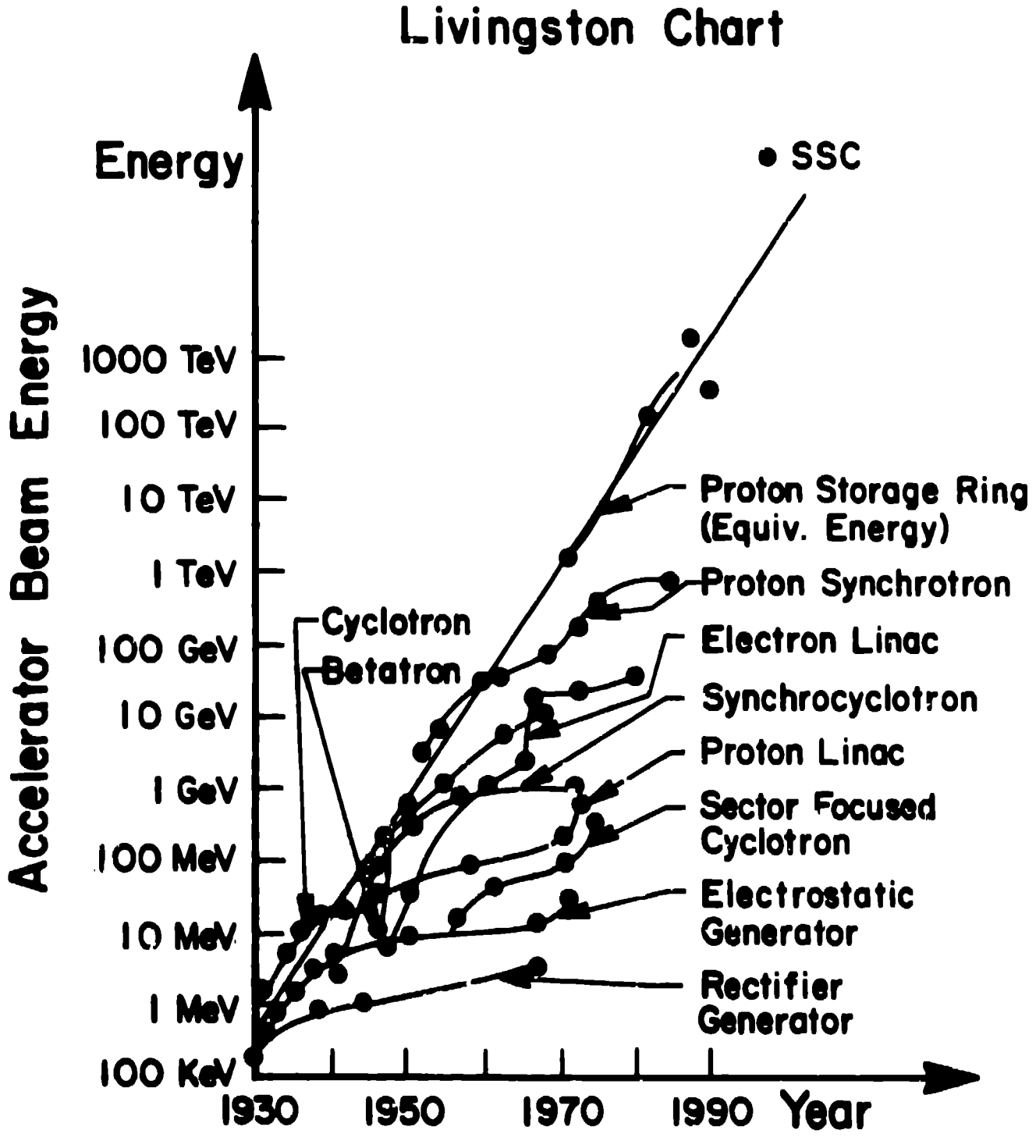
Livingston Chart
Energy
Accelerator Beam Energy
1000 TeV
100 TeV
10 TeV
1 TeV
100 GeV
10 GeV
1 GeV
100 MeV
10 MeV
1 MeV
100 KeV
1930
1950
1970
1990
Year
SSC
Proton Storage Ring
(Equiv. Energy)
Proton Synchrotron
Electron Linac
Synchrocyclotron
Proton Linac
Sector Focused
Cyclotron
Electrostatic
Generator
Rectifier
Generator
Cyclotron
Betatron

Fig 1

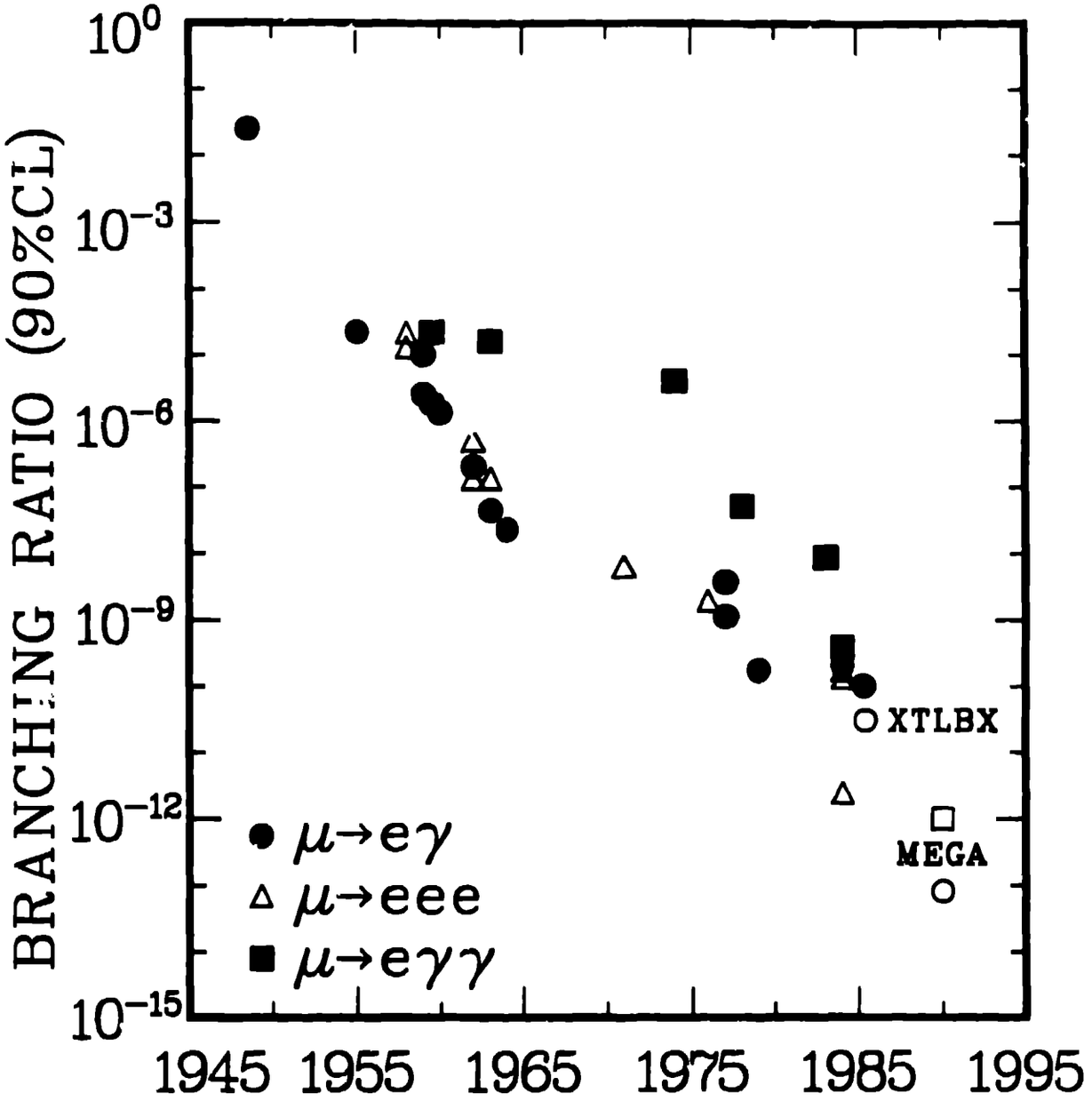
BRANCHING RATIO (90%CL)
10^{0}
10^{-3}
10^{-6}
10^{-9}
10^{-12}
10^{-15}
1945
1955
1965
1975
1985
1995
● $\mu \to e\gamma$
△ $\mu \to eee$
■ $\mu \to e\gamma\gamma$
XTLBX
MEGA

Figure 2

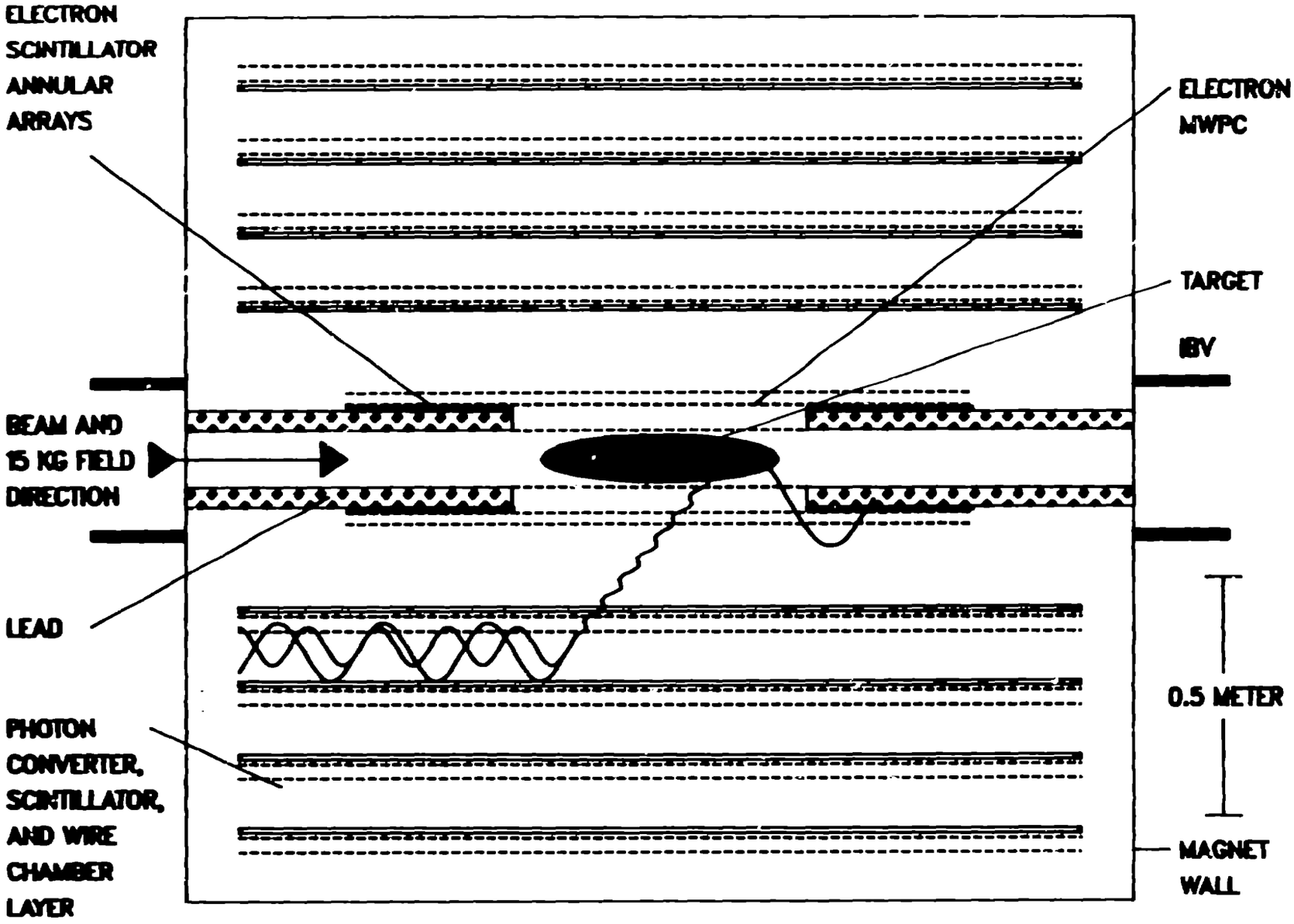
ELECTRON SCINTILLATOR ANNULAR ARRAYS
ELECTRON MWPC
TARGET
IBV
BEAM AND 15 KG FIELD DIRECTION
LEAD
PHOTON CONVERTER, SCINTILLATOR, AND WIRE CHAMBER LAYER
0.5 METER
MAGNET WALL

Fig 3

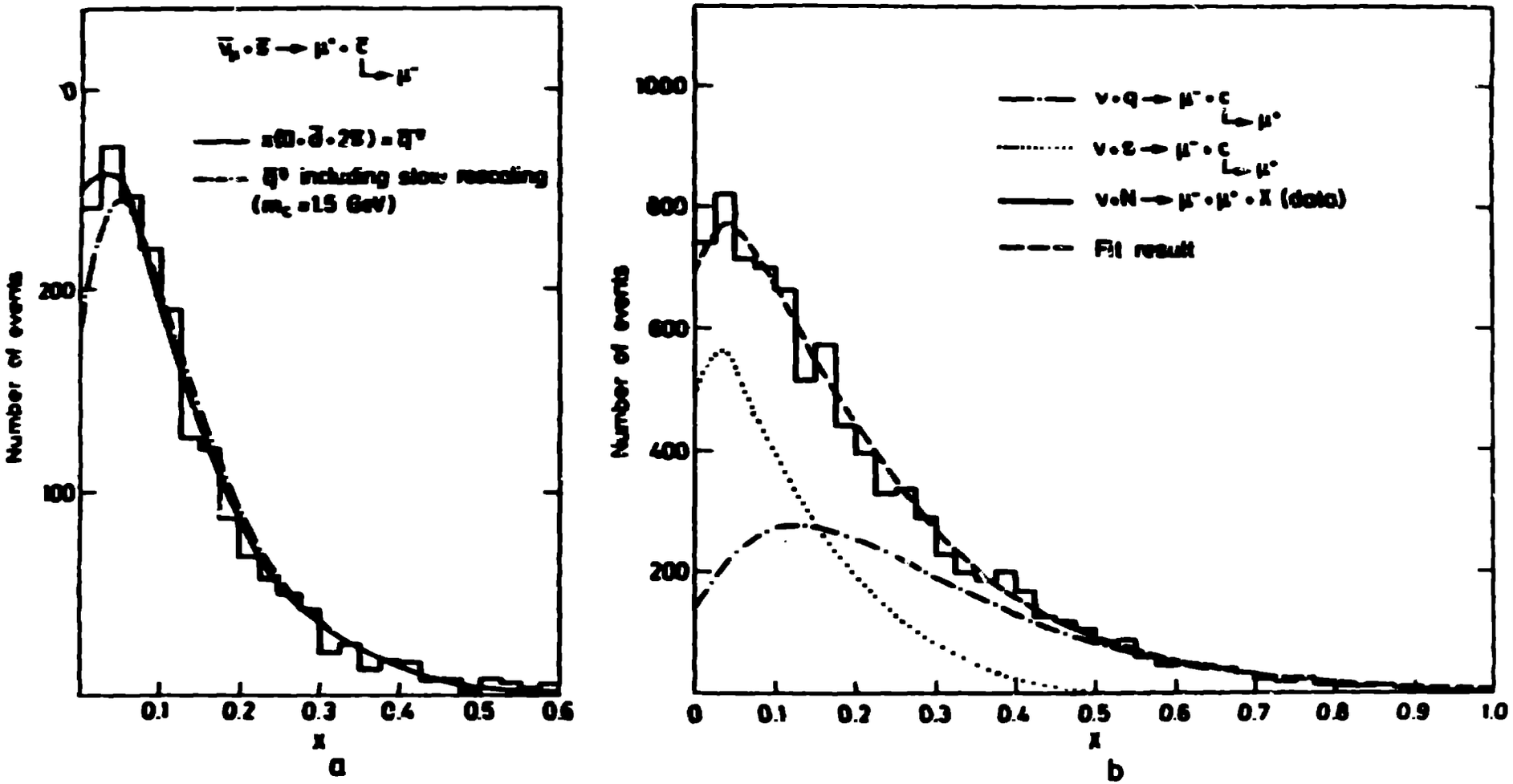

Fig 1

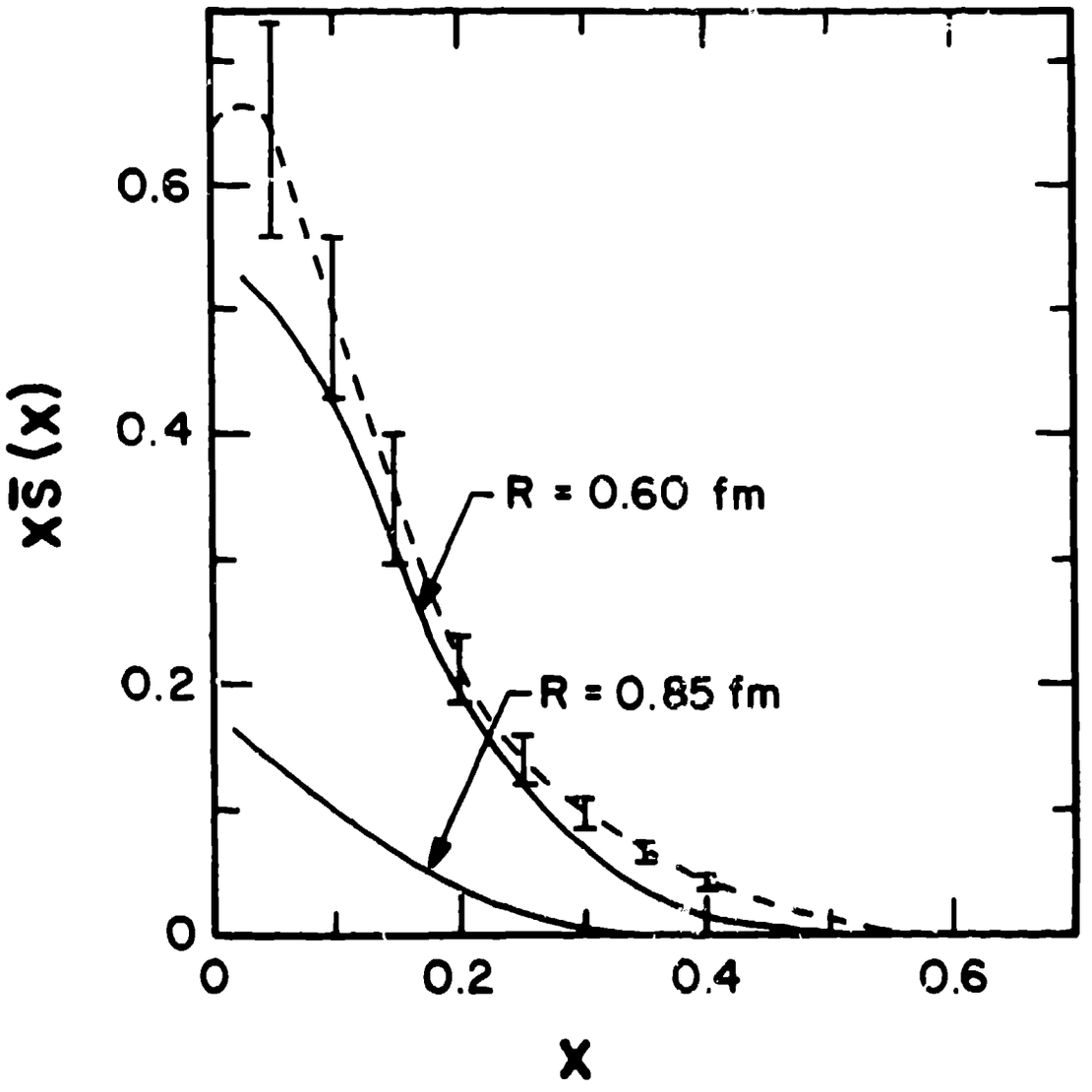

Fig 5a

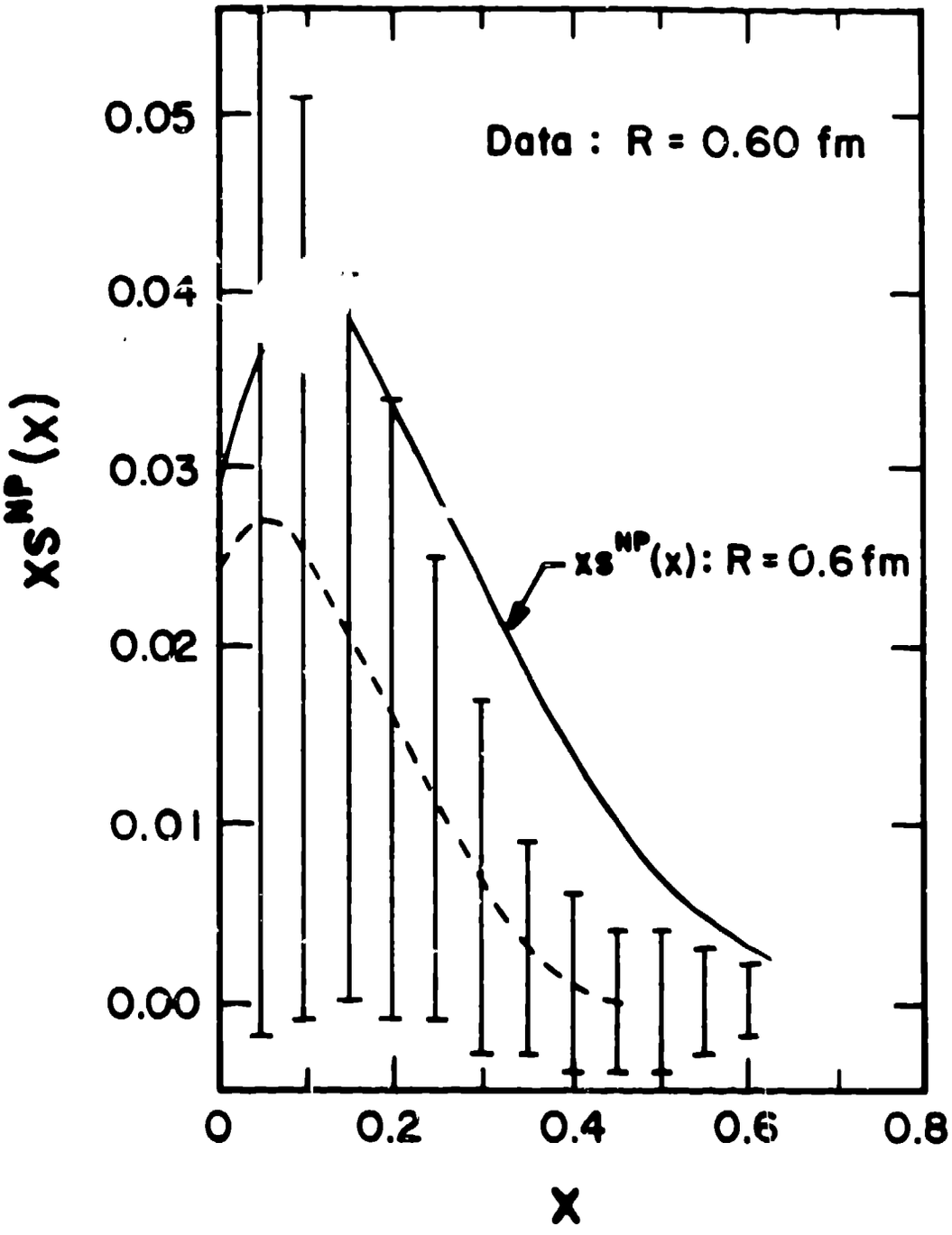
Data : R = 0.60 fm
$xs^{NP}(x)$: R = 0.6 fm
$xS^{NP}(x)$
0.05
0.04
0.03
0.02
0.01
0.00
0
0.2
0.4
0.6
0.8
X

Fig 5b

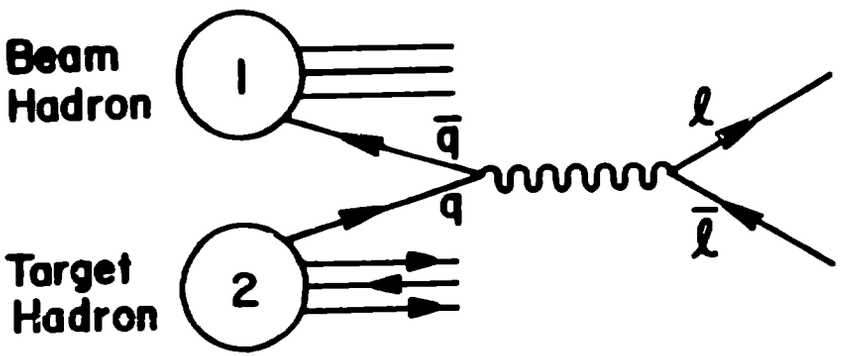

Fig 6

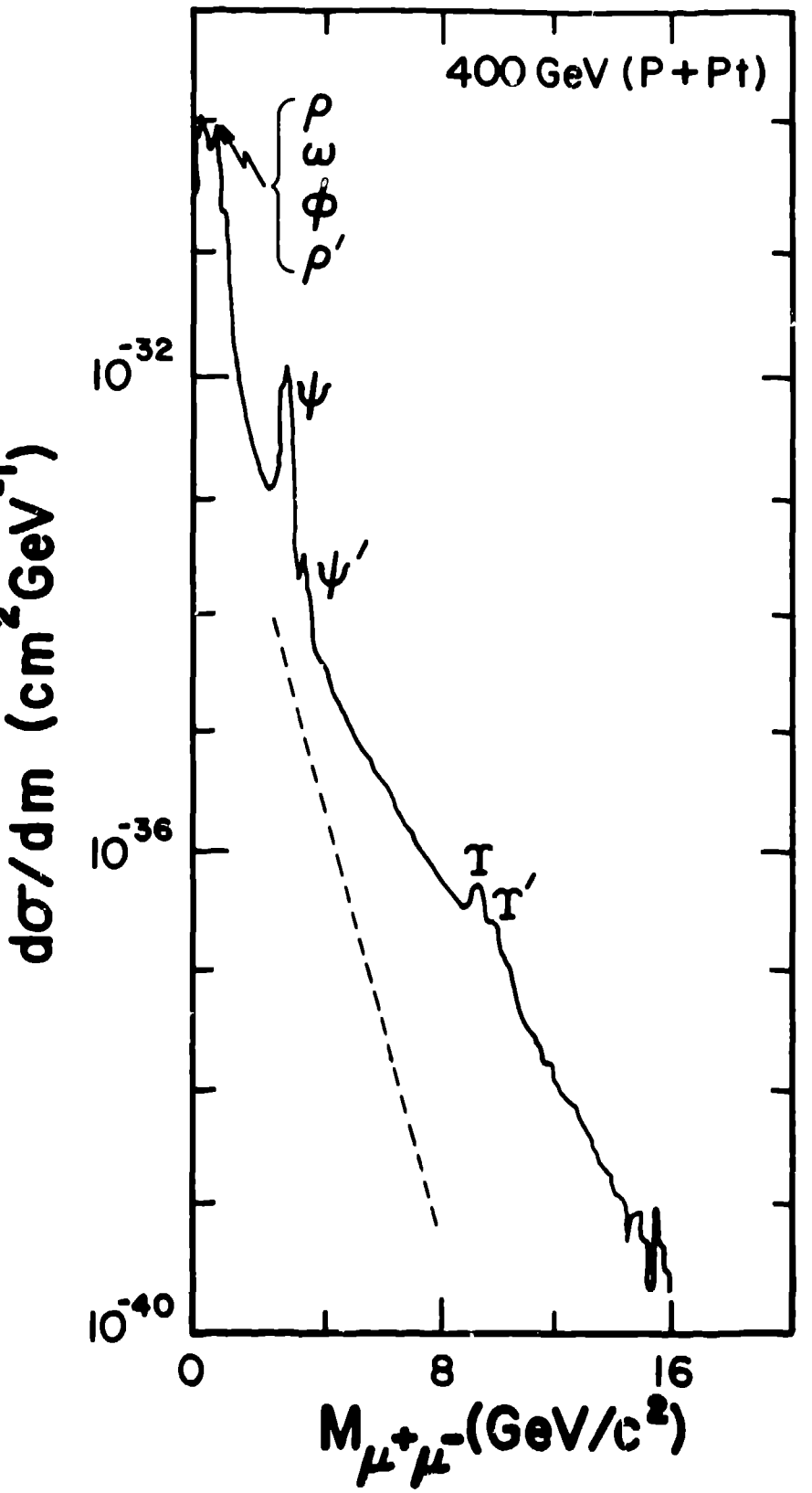
400 GeV (P + Pt)
ρ
ω
φ
ρ′
ψ
ψ′
Υ
Υ′
10^-32
10^-36
10^-40
dσ/dm (cm^2 GeV^-1)
0
8
16
M_μ+μ- (GeV/c^2)

Fig 7

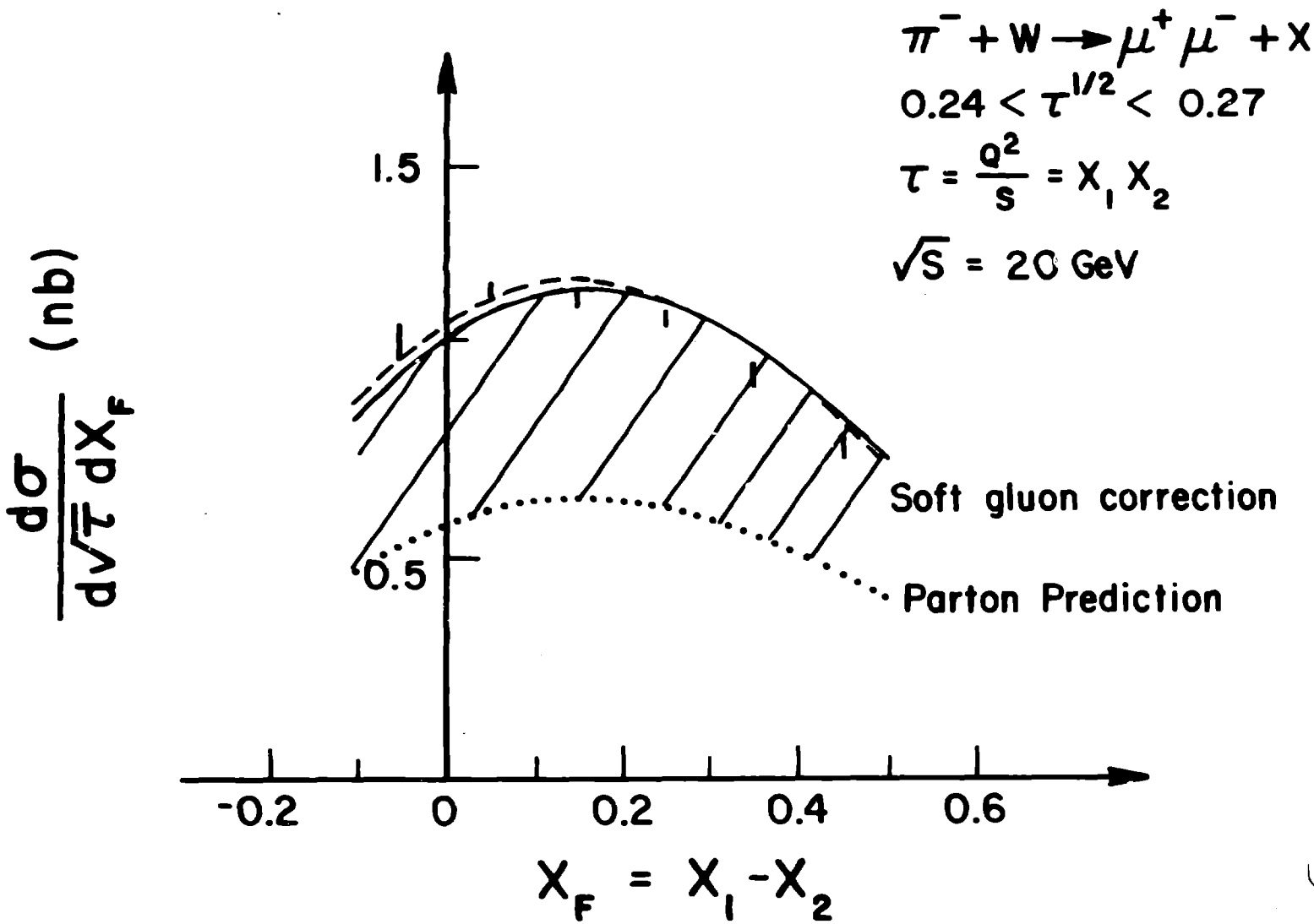
$\pi^- + W \rightarrow \mu^+ \mu^- + X$
$0.24 < \tau^{1/2} < 0.27$
$\tau = \frac{q^2}{s} = X_1 X_2$
$\sqrt{s}$ = 20 GeV
$\frac{d\sigma}{d\sqrt{\tau}\, dX_F}$ (nb)
1.5
1
0.5
Soft gluon correction
Parton Prediction
-0.2
0
0.2
0.4
0.6
$X_F = X_1 - X_2$

Fig 8

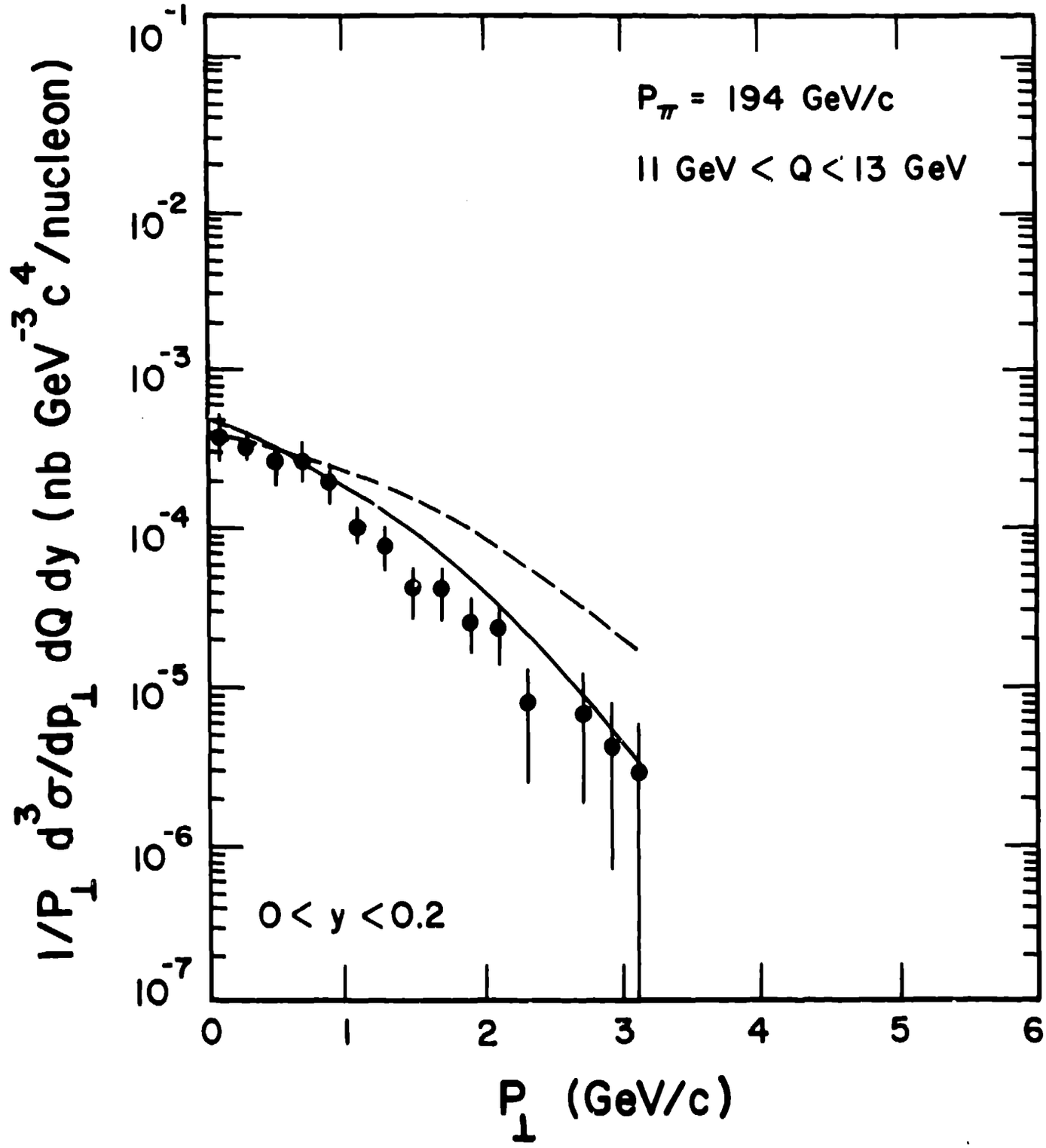
P_π = 194 GeV/c
11 GeV < Q < 13 GeV
0 < y < 0.2
$1/P_\perp \, d^3\sigma/dp_\perp \, dQ \, dy$ (nb GeV^{-3}c^4/nucleon)
$P_\perp$ (GeV/c)
10^{-1}
10^{-2}
10^{-3}
10^{-4}
10^{-5}
10^{-6}
10^{-7}
0
1
2
3
4
5
6

Fig 5

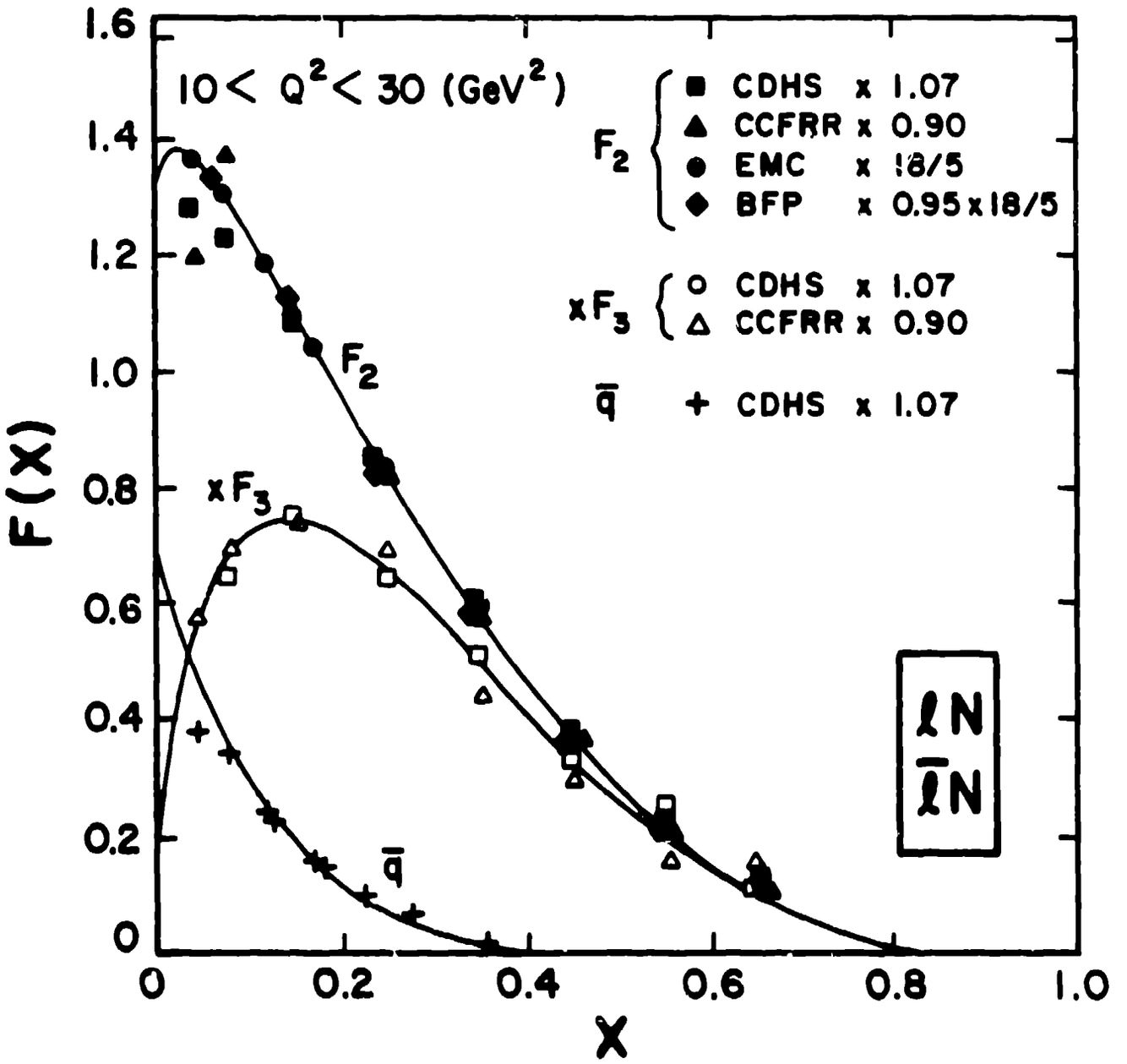
10< Q²< 30 (GeV²)
F₂
■ CDHS x 1.07
▲ CCFRR x 0.90
● EMC x 18/5
◆ BFP x 0.95 x 18/5
xF₃
○ CDHS x 1.07
△ CCFRR x 0.90
q̄ + CDHS x 1.07
F₂
xF₃
q̄
ℓN
ℓ̄N
F(X)
X
0
0.2
0.4
0.6
0.8
1.0
1.2
1.4
1.6

Fig 10

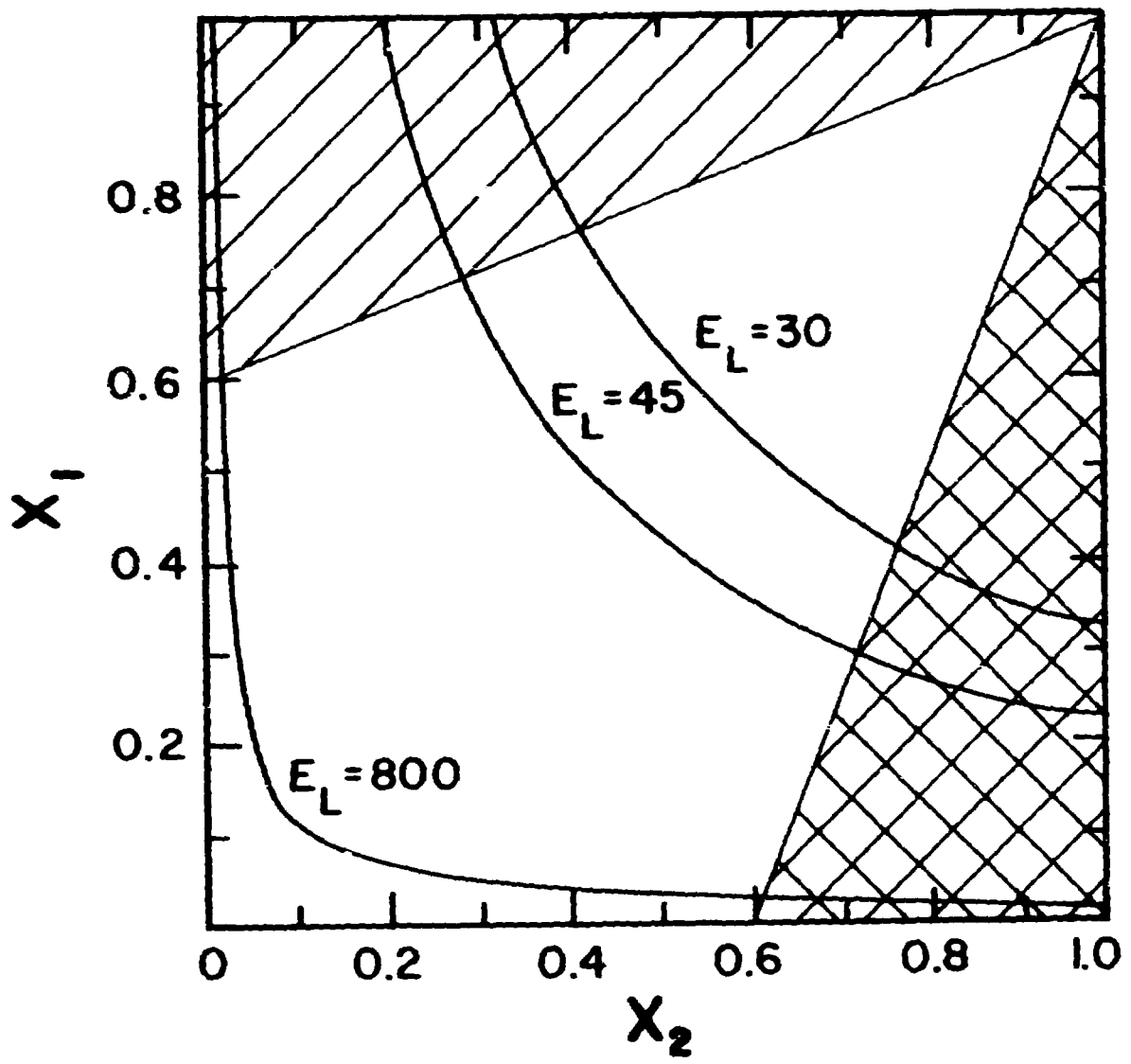

Fig 11

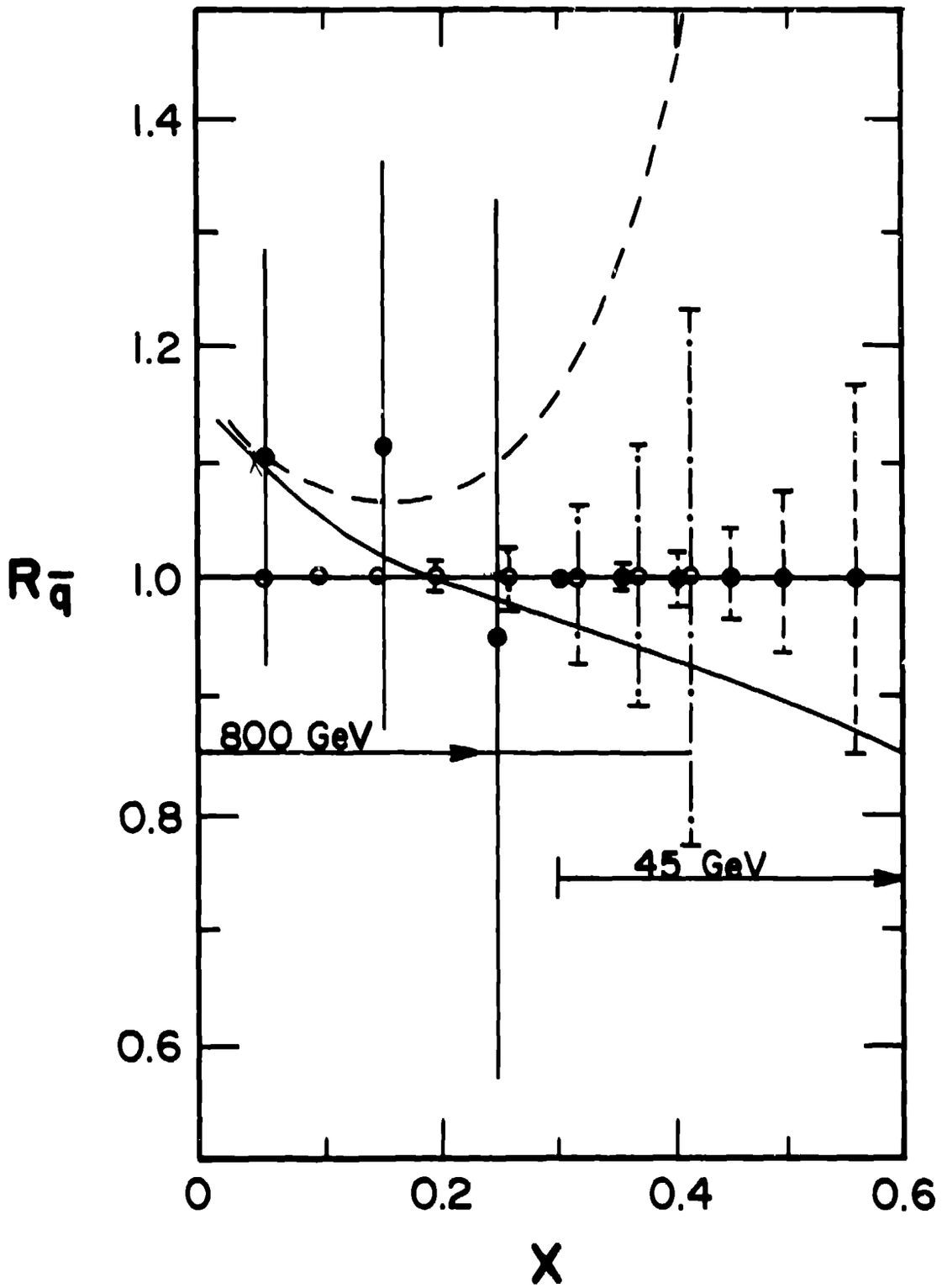

Fig 12

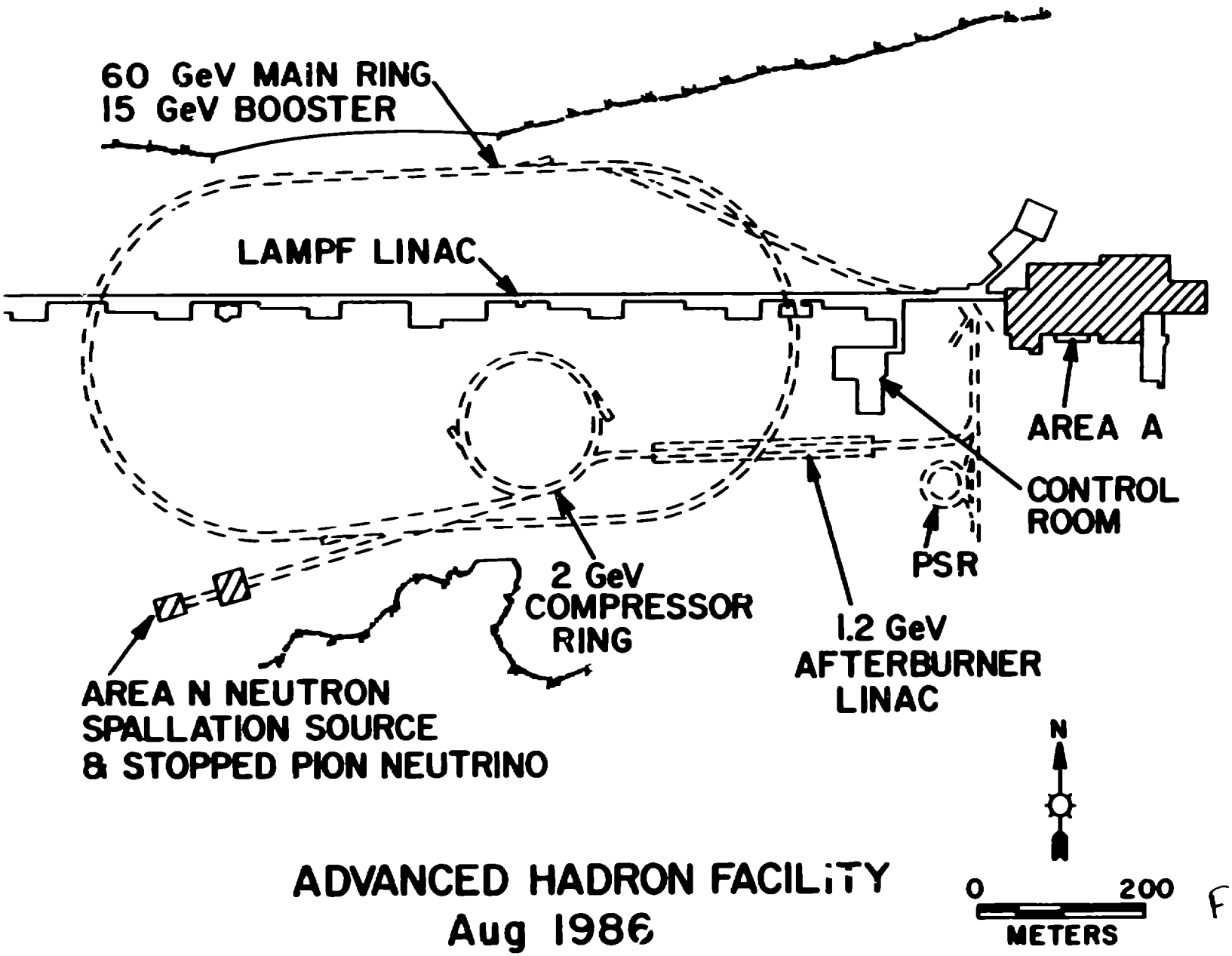

ADVANCED HADRON FACILITY
Aug 1986

Fig 13